American Mineralogist, Volume 79, pages 175–184, 1994

Maricopaite, an unusual lead calcium zeolite with an interrupted mordenite-like framework and intrachannel Pb_4 tetrahedral clusters

ROLAND C. ROUSE, DONALD R. PEACOR
Department of Geological Sciences, University of Michigan, Ann Arbor, Michigan 48109-1063, U.S.A.

ABSTRACT

The zeolite mineral maricopaite $[Pb_7Ca_2Al_{12}Si_{36}(O,OH)_{100} \cdot n(H_2O,OH)]$ is orthorhombic, *Cm2m*, with $a = 19.434(2)$, $b = 19.702(2)$, $c = 7.538(1)$ Å, $V = 2886.1(7)$ Å^3, and $Z = 1$. The measured and calculated densities are 2.94 and 2.90 g/cm^3, respectively. The crystal structure, which was solved by direct methods and refined to an unweighted residual of 0.046 for 1189 observed reflections, is based on an interrupted mordenite-like framework in which 17% of the TO_4 groups are threefold connected. The maricopaite framework differs from that of mordenite in the following respects: (1) The four- and eight-membered rings in mordenite do not exist in maricopaite due to framework interruptions. (2) The elliptical eight-membered-ring channels ‖ **c** in mordenite become cruciform 12-membered-ring channels in maricopaite. (3) The short channels ‖ **b** in mordenite are absent in maricopaite. (4) The elliptical 12-membered-ring channels ‖ **c** in mordenite also exist in maricopaite, but access between them and the cruciform channels in the **b** direction is through single eight-membered-ring ports, rather than through short connecting channels ‖ **b**, as in mordenite. The cruciform channels are obstructed by $Pb_4(O,OH)_4$ clusters in which the Pb atoms form Pb_4 tetrahedra, each tetrahedron face being capped by an O or OH ligand. All Pb sites are partially occupied, and there are two alternative sites for each Pb_4 tetrahedron, sites that cannot be simultaneously occupied due to short Pb-Pb distances. The observed Pb-Pb distances range from 3.584(4) to 3.954(4) Å.

INTRODUCTION

In 1988 a new hydrated lead calcium aluminosilicate, maricopaite, from the Moon Anchor mine, near Tonopah, Maricopa County, Arizona, was described by Peacor et al. Maricopaite occurs as a secondary mineral in a single calcite-fluorite vein, where it coats and fills fractures in quartz and is closely associated with mimetite. The remainder of the secondary mineral assemblage present consists of arsenates, chromates, carbonates, and silicates of Pb, Ca, and Cu, namely cerrusite, fornacite, phoenicochroite, duftite, chrysocolla, and wickenburgite. Peacor et al. noted that the chemical composition, unit-cell parameters, symmetry, and infrared absorption spectrum of maricopaite all resembled those of the zeolite mineral mordenite ($Na_3KCa_2Al_8Si_{40}O_{96} \cdot 28H_2O$), but that the provisional formula $[Pb_7Ca_2(Al,Si)_{48}O_{100} \cdot 32H_2O]$ had a T:O ratio slightly less than that of a tektosilicate. On the basis of these considerations, they hypothesized that maricopaite is either a zeolite or a zeolite-like compound, with a structure closely related to that of mordenite.

An analysis of the crystal structure, the results of which are reported here, has verified the interpretation proposed by Peacor et al. (1988). Maricopaite is essentially a derivative of the mordenite structure but is not a true tektosilicate, the T-O-T linkages of its mordenite-like framework being interrupted at several points by unshared O vertices. Maricopaite therefore joins a small group of natural and synthetic compounds having interrupted tetrahedral framework structures. Smith (1988) listed ten aluminosilicates and beryllosilicates plus one aluminophosphate in this category. A gallophosphate (Estermann et al., 1991), a beryllophosphate (Harrison et al., 1991), and two zincophosphates (Harrison et al., 1992), all with interrupted frameworks, have subsequently been described.

STRUCTURE SOLUTION AND REFINEMENT

Most crystals of maricopaite are quite imperfect and unsuitable for intensity data measurement. The specimen selected for structure analysis was a euhedral, acicular crystal, which proved adequate for the purpose despite extensive streaking of reflections in the ω direction in the low-θ region. The crystal was first studied by the Weissenberg method, with levels 0–3 normal to the **c** axis being photographed using Cu$K\alpha$ radiation and 48–60 h exposure times. The photographs confirmed the cell parameters and possible space groups reported by Peacor et al. (1988), except that **a** and **b** of their cell were interchanged to conform to the convention $b > a > c$ for orthorhombic crystals. In the new setting, the possible space groups are *Cmmm*, *Cm2m*, *Cmm2*, or *C222*, but, since all reflections $h0l$ with l odd are very weak or unobserved, maricopaite has *Cmcm*, *C2cm*, or $Cmc2_1$ pseudosymmetry.

0003–004X/94/0102–0175$02.00

TABLE 1. Experimental details

Crystal size	0.047 × 0.063 × 0.266 mm
Radiation	monochromatized Mo$K\alpha$ (λ = 0.7107 Å)
Reflection scans	
Scan type	ω-2θ
Scan rates	between 0 and 7°/min in ω
Scan widths	0.62 + 0.350 (tan θ) in ω
Data measured	54.90°
Maximum 2θ	1873
Reflections measured	1873
Unique reflections	1189 with $I_{obs} \geq 3\sigma(I_{obs})$
Observed reflections	3 standard reflections every 3 h
Intensity monitoring	3 standard reflections every 400 reflections
Orientation monitoring	
Data corrections	applied
Lorentz and polarization	ψ-scan method using 8 reflections followed by Fourier method (Walker and Stuart, 1983)
Absorption	not applied
Extinction	by direct methods using the Multan 11/82 package
Structure solution	
Structure refinement	full-matrix least squares
Type	$\Sigma w(\lvert F_{obs}\rvert - \lvert F_{calc}\rvert)^2$
Function minimized	$4F^2_{obs}/\sigma^2(F^2_{obs})$
Weighting function	for all atoms
Anomalous dispersion	1189 reflections
Observations	180 refined parameters
Variables	0.046
R (observed data)	0.051
R_w (observed data)	0.137
R (all data)	1.968
Esd of obs. of unit wt.	1.4(2) e/Å^3 (on final map)
Largest $\Delta\rho(x,y,z)$	Enraf-Nonius CAD4
Diffractometer	
Computation	MicroVAX 3100
Hardware	MolEN crystallographic software system
Software	

The crystal was mounted on an Enraf-Nonius CAD4 four-circle diffractometer, and its unit-cell parameters were refined by least squares from the measured setting angles of 18 reflections, yielding a = 19.434(2), b = 19.702(2), c = 7.538(1) Å, and V = 2886.1(7) Å^3. A second refinement using 12 reflections from the powder data of Peacor et al. (1988), with additional higher θ reflections indexed with the aid of the structure factors, yielded a = 19.385(3), b = 19.713(4), c = 7.522(2) Å, and V = 2874.2(8) Å^3. The calculated densities based upon the simplified unit cell contents $Pb_7Ca_2Al_{12}Si_{36}O_{100}\cdot 32H_2O$ are 2.90 (with the cell volume from the diffractometer data refinement) and 2.91 g/cm^3 (with the cell volume from the powder data refinement). These values are less than the measured value of 2.94 g/cm^3, but both are necessarily slightly low, owing in part to the fact that the contribution from the minor organic component of unknown identity reported in the chemical analysis of Peacor et al. (1988) is neglected.

The intensities of 1873 reflections constituting one asymmetric unit were measured with the CAD4 and converted to structure factor amplitudes by correction for Lorentz-polarization and absorption effects. The latter correction was applied by the ψ-scan method of North et al. (1968), and a supplementary absorption correction was later applied using the method of Walker and Stuart (1983), after completion of the structure refinement with isotropic displacement factors. Of the 1873 reflections in the data set, 1189 were considered observed. Additional information concerning data measurement and reduction is presented in Table 1. All computations involving data reduction and the solution and refinement of the structure were carried out using the Enraf-Nonius crystallographic software system MolEN.

Analysis of the Patterson function revealed two probable Pb atom sites and the probable space group, $Cm2m$ (standard setting $Amm2$), which eventually proved to be the correct choice. The locations of all framework cations (eight T sites), all extraframework cations (four Pb sites), nine of the 18 framework anion sites, and one of the ten extraframework anion sites were obtained by direct methods, utilizing the Multan 11/82 package incorporated in MolEN. The remaining nine framework anion sites were found simply by placing atoms midway between adjacent T sites and allowing least squares to shift them to their proper locations. The remaining nine extraframework anion sites, the validity of which is not above question, were located using difference electron density syntheses. No separate site for the ~2 Ca reported in the chemical analysis could be located, and the Ca are assumed to be disordered over multiple extraframework sites for reasons given below. The apparent solid solution of Al and Si in the framework was treated by assuming a uniform distribution of the 11.6 Al and 36.4 Si, indicated by the chemical analysis (Peacor et al., 1988) over the eight T sites.

It became evident from calculations of interatomic distances and site occupancy factor refinements that none of the extraframework sites was fully occupied by Pb or H_2O. Whereas it was possible to refine both total site occupancy and displacement factors simultaneously for the Pb sites, that was not the case for the H_2O positions, owing to high correlations between these two parameters. The displacement factors of the H_2O sites were therefore fixed at the average isotropic B of the framework anions (2.6 Å^2), and the occupancy factors were then refined.

Refinement using isotropic displacement factors for all atoms converged at an unweighted residual of 0.076. Conversion to anisotropic displacement factors for all framework atoms plus O19w reduced the residual to 0.049, but displacement factors of six of the 19 anions were nonpositive definite, a result not unexpected given the very small contribution to the intensities by the anions in a given site relative to those of the cations (especially Pb). All anions were therefore refined with isotropic displacement factors for the remainder of the refinement. A second problem was the behavior of T5, which occasionally became nonpositive definite during subsequent cycles. This problem was solved by assuming T5 to be occupied entirely by Si and redistributing the remaining 11.6 Al and 32.4 Si uniformly over the other seven T sites.

At this point a listing of reflections having the largest values of $\lvert F\rvert_{obs} - \lvert F\rvert_{calc}$ revealed five reflections (110, 200, 001, 130, and 310) having low θ values [(sin θ)/$\lambda \leq$

TABLE 3. Atomic parameters for maricopaite

Site	Equipoint	*x*	*y*	*z*	B_{iso} (Å²)	Occupancy
Pb1	4*e*	0.0975(1)	0.1044	½	2.25(2)	3.32(1)
Pb2	4*d*	0.0977(2)	0.8988(2)	0	1.83(8)	0.98(1)
Pb3	4*c*	0	0.9662(1)	0.2377(2)	2.29(3)	2.49(1)
Pb4	4*c*	0	0.0359(3)	0.2516(11)	3.4(2)	0.70(1)
T1	8*f*	0.1790(3)	0.2907(2)	0.2956(6)	1.17(9)	
T2	8*f*	0.3211(3)	0.2169(2)	0.2043(6)	1.38(9)	
T3	8*f*	0.2546(3)	0.9283(2)	0.2076(6)	1.18(9)	
T4	4*e*	0.1395(3)	0.9238(3)	½	1.0(1)	
T5	4*d*	0.1342(4)	0.0843(3)	0	1.1(1)	
T6	8*f*	0.2554(3)	0.0779(2)	0.2885(6)	1.26(9)	
T7	4*d*	0.0794(4)	0.2311(3)	0	1.6(1)	
T8	4*e*	0.0817(3)	0.7763(3)	½	1.1(1)	
O1	8*f*	0.1861(7)	0.9200(6)	0.3250(18)	2.9(3)	
O2	4*d*	0.0810(9)	0.1441(9)	0	2.3(4)	
O3	4*e*	0.0932(11)	0.9916(11)	½	3.8(5)	
O4	4*e*	0.0862(8)	0.8586(8)	½	1.4(3)	
O5	4*d*	0.3443(9)	0.2307(8)	0	2.2(4)	
O6	8*f*	0.1820(6)	0.0864(5)	0.1811(16)	1.7(2)	
O7	8*f*	0.3134(6)	0.1342(5)	0.2417(16)	2.3(2)	
O8	4*e*	0.1607(11)	0.2769(10)	½	3.5(5)	
O9	4*d*	0.0863(10)	0.0162(9)	0	2.4(4)	
O10	8*f*	0.1865(6)	0.3708(6)	0.2641(16)	2.0(2)	
O11	8*f*	0.2500(9)	0.2536(9)	0.2506(24)	3.6(3)	
O12	8*f*	0.1164(6)	0.2604(7)	0.1761(19)	3.0(3)	
O13	8*f*	0.3832(7)	0.2424(6)	0.3218(20)	3.3(3)	
O14	8*f*	0.2897(6)	0.0030(7)	0.2460(22)	2.5(2)	
O15	4*d*	0.2278(10)	0.9219(9)	0	2.5(4)	
O16	4*e*	0.2340(9)	0.0838(8)	½	2.0(4)	
O17	2*a*	0	0.2530(14)	0	2.5(5)	
O18	2*b*	0	0.7557(14)	½	2.6(5)	
O19w	4*c*	0	0.0828(9)	0.3098(27)	2.2(4)	3.7(1)
O20w	2*b*	0	0.231(1)	½	2.6	1.9(1)
O21w	4*d*	0.085(2)	0.561(1)	0	2.6	2.4(1)
O22w	4*c*	0	0.501(2)	0.099(5)	2.6	2.0(1)
O23w	4*e*	0.061(3)	0.594(3)	½	2.6	1.1(1)
O24w	8*f*	0.077(4)	0.456(3)	0.241(10)	2.6	1.4(2)
O25w	8*f*	0.074(3)	0.457(3)	0.385(9)	2.6	1.6(2)
O26w	4*d*	0.079(2)	0.871(2)	0	2.6	2.3(1)
O27w	4*e*	0.070(6)	0.151(6)	½	2.6	0.7(1)
O28w	4*c*	0	0.933(2)	0.215(5)	2.6	1.9(2)

Note: the temperature factors given for all cations are equivalent isotropic *B*, as these atoms were refined with anisotropic displacement factors. The displacement factors of O20w through O28w were fixed at 2.6 Å², and the *y* coordinate of Pb1 was fixed at 0.1044 to define the origin along **b**. The refined occupancies listed are in atoms per cell. Estimated standard deviations for all parameters are in parentheses.

0.08], medium to high intensities, and $|F|_{obs} \ll |F|_{calc}$. These features normally indicate the presence of extinction factors in the intensity data, but that seems quite improbable in this case, given the pronounced mosaic structure of the crystal so evident in the Weissenberg photographs. Nevertheless, the five reflections in question were excluded from the remainder of the refinement but retained in the data set.

The refinement of the maricopaite structure finally converged at an unweighted residual of 0.046. Additional details concerning the structure solution and refinement process are given in Table 1. Table 2[1] contains a list of structure factors, Table 3 the refined atomic parameters, Table 4[1] the anisotropic displacement factors, and Table 5 selected interatomic distances and angles.

[1] Copies of Tables 2 and 4 may be ordered as Document AM-94-545 from the Business Office, Mineralogical Society of America, 1130 Seventeenth Street NW, Suite 330, Washington, DC 20036, U.S.A. Please remit $5.00 in advance for the microfiche.

STRUCTURE DESCRIPTION AND DISCUSSION

Comparison of maricopaite and mordenite frameworks

The crystal structure of maricopaite is essentially a distorted derivative of the well-known structure of mordenite. The latter was originally solved by Meier (1961), and the structures of mordenite samples having a variety of exchangeable cations and hydration states have subsequently been refined (e.g., Ito and Saito, 1985; Alberti et al., 1986; Elsen et al., 1987). The chief difference between these structures and that of maricopaite lies in the incomplete (interrupted) tectosilicate framework of the latter; i.e., 17% of the TO_4 groups in maricopaite are threefold connected rather than fourfold connected, with the unshared vertex anions satisfying their valence requirements by bonding to extraframework Pb atoms. The Zoltai sharing coefficient for the framework is 1.833, which is comparable with the lowest values among the ten natural and synthetic compounds with interrupted frameworks listed by Smith (1988). The framework density of maricopaite is 16.6 T per 1000 Å³, which is 4% lower

TABLE 5. Selected interatomic distances (Å) and angles (°) for maricopaite

Pb-O and Pb-Ow			
Pb1-O3	2.22(2)	Pb3-O19w	2.36(2)
-O19w	2.41(1) × 2	-O9	2.64(1) × 2
-O16	2.68(2) × 2	-O3	2.73(1) × 2
-O6	2.93(1) × 2	-O26w	3.02(3) × 2
-O20w	3.13(2)	Mean	2.73
Mean	2.67		
Pb2-O9	2.32(2)	Pb4-O28w	2.04(4)
-O15	2.57(2)	-O9	2.56(1) × 2
-O28w	2.59(3) × 2	-O3	2.75(2) × 2
-O1	3.02(1) × 2	-O27w	3.24(9) × 2
Mean	2.68	Mean	2.73
T-O and O-T-O			
T1-O11	1.60(2)	O8-T1-O12	107.7(9)
-O10	1.60(1)	O8-T1-O11	108.5(10)
-O8	1.60(1)	O8-T1-O10	109.2(8)
-O12	1.63(1)	O10-T1-O11	109.9(8)
Mean	1.61	O10-T1-O12	110.3(7)
		O11-T1-O12	111.1(8)
		Mean	109.5
T2-O13	1.58(1)	O5-T2-O13	105.4(9)
-O11	1.60(2)	O7-T2-O13	106.6(7)
-O5	1.63(1)	O7-T2-O11	109.2(8)
-O7	1.66(1)	O5-T2-O7	110.5(8)
Mean	1.62	O5-T2-O11	111.7(9)
		O11-T2-O13	113.3(9)
		Mean	109.5
T3-O1	1.61(1)	O1-T3-O15	104.6(8)
-O14	1.65(1)	O10-T3-O14	106.2(6)
-O15	1.65(1)	O1-T3-O14	109.7(7)
-O10	1.66(1)	O1-T3-O10	111.0(7)
Mean	1.64	O14-T3-O15	111.4(9)
		O10-T3-O15	114.0(8)
		Mean	109.5
T4-O1	1.60(1)	O3-T4-O4	107.2(10)
-O1	1.60(1)	O1-T4-O4	108.6(6)
-O3	1.61(2)	O1-T4-O4	108.6(6)
-O4	1.65(2)	O1-T4-O3	110.7(6)
Mean	1.62	O1-T4-O3	110.7(6)
		O1-T4-O1	110.9(11)
		Mean	109.5
T5-O2	1.57(2)	O2-T5-O9	104.0(10)
-O9	1.63(2)	O6-T5-O9	109.9(5)
-O6	1.65(1)	O6-T5-O9	109.9(5)
-O6	1.65(1)	O2-T5-O6	110.7(5)
Mean	1.62	O2-T5-O6	110.7(5)
		O6-T5-O6	111.4(9)
		Mean	109.4
T6-O7	1.62(1)	O6-T6-O16	104.4(8)
-O6	1.65(1)	O7-T6-O14	106.8(6)
-O14	1.65(1)	O7-T6-O16	109.7(7)
-O16	1.65(1)	O6-T6-O14	110.2(6)
Mean	1.64	O14-T6-O16	110.6(8)
		O6-T6-O7	115.2(6)
		Mean	109.5
T7-O17	1.60(1)	O2-T7-O17	106.6(12)
-O12	1.62(1)	O12-T7-O17	109.5(7)
-O12	1.62(1)	O12-T7-O17	109.5(7)
-O2	1.72(2)	O12-T7-O12	110.4(10)
Mean	1.64	O2-T7-O12	110.4(6)
		O2-T7-O12	110.4(6)
		Mean	109.5
T8-O4	1.62(2)	O4-T8-O18	107.4(12)
-O18	1.64(1)	O13-T8-O18	107.5(7)
-O13	1.65(1)	O13-T8-O18	107.5(7)
-O13	1.65(1)	O13-T8-O13	109.2(10)
Mean	1.64	O4-T8-O13	112.5(6)
		O4-T8-O13	112.5(6)
		Mean	109.4

TABLE 5.—*Continued*

T-T and T-O-T			
T1-T3	3.075(6)	T1-O10-T3	140(1)
-T1	3.082(10)	T1-O8-T1	148(1)
-T7	3.176(7)	T1-O12-T7	157(1)
-T2	3.197(7)	T1-O11-T2	180(2)
Mean	3.132	Mean	156
T2-T2	3.080(10)	T2-O5-T2	142(1)
-T6	3.088(6)	T2-O7-T6	140(1)
-T8	3.147(7)	T2-O13-T8	154(1)
-T1	3.197(7)	T2-O11-T1	180(2)
Mean	3.128	Mean	154
T3-T6	3.010(6)	T3-O14-T6	132(1)
-T1	3.075(6)	T3-O10-T1	140(1)
-T3	3.129(9)	T3-O15-T3	142(1)
-T4	3.142(7)	T3-O1-T4	157(1)
Mean	3.089	Mean	143
T4-T8	3.115(9)	T4-O4-T8	144(1)
-T3	3.142(7)	T4-O1-T3	157(1)
-T3	3.142(7)	T4-O1-T3	157(1)
Mean	3.133	Mean	153
Pb1	3.652(7)	T4-O3-Pb1	144(1)
T5-T7	3.082(9)	T5-O2-T7	140(1)
-T6	3.209(7)	T5-O6-T6	153(1)
-T6	3.209(7)	T5-O6-T6	153(1)
Mean	3.167	Mean	149
Pb2	3.723(7)	T5-O9-Pb2	140(1)
T6-T3	3.010(6)	T6-O14-T3	132(1)
-T2	3.088(6)	T6-O7-T2	140(1)
-T6	3.188(10)	T6-O16-T6	150(1)
-T5	3.209(7)	T6-O6-T5	153(1)
Mean	3.124	Mean	144
T7-T5	3.082(9)	T7-O2-T5	140(1)
-T7	3.085(14)	T7-O17-T7	149(2)
-T1	3.176(7)	T7-O12-T1	157(1)
-T1	3.176(7)	T7-O12-T1	157(1)
Mean	3.130	Mean	151
T8-T4	3.115(9)	T8-O4-T4	144(1)
-T2	3.147(7)	T8-O13-T2	154(1)
-T2	3.147(7)	T8-O13-T2	154(1)
-T8	3.176(13)	T8-O18-T8	151(2)
Mean	3.146	Mean	151
$Pb1_2Pb3_2$ tetrahedron		$Pb2_2Pb4_2$ tetrahedron	
Pb1-Pb1	3.788(3)	Pb2-Pb2	3.798(9)
Pb1-Pb3	3.862(2) × 4	Pb2-Pb4	3.808(7) × 4
Pb3-Pb3	3.954(4)	Pb4-Pb4	3.792(16)
Mean	3.865	Mean	3.804
Pb3-Pb3 (between tetrahedra)	3.584(4)	Pb4-Pb4 (between tetrahedra)	3.745(16)

Note: estimated standard deviations are in parentheses.

than the corresponding value of 17.3 for natural Ca-exchanged mordenite (Elsen et al., 1987).

The basic similarity of the mordenite and maricopaite structures, as well as their substantial differences in detail, are evident in Figures 1–4. Note that the origin of the maricopaite cell should be shifted by ½ along [100] to facilitate the comparison. The complete (but approximate) coordinate transformation applicable to the framework sites in the two structures is $x_{mor} = x_{mar} + ½$, $y_{mor} = y_{mar}$, $z_{mor} = z_{mar} - ¼$. The O3 and O9 atoms of maricopaite are exceptions to this rule, as they are the unshared tetrahedral anions, whose positions differ greatly from those in a fully connected framework. In addition, many of the occupied extraframework sites in maricopaite roughly approximate standard extraframework sites in mordenite (designated A, B, C . . . J). The relationships between the tetrahedral frameworks of mordenite and maricopaite will be elucidated using the structure of Ca-rich mordenite (Elsen et al., 1987) as a representative example of the numerous compositional varieties of this mineral. Chemical and crystallographic data for Ca-rich mordenite and maricopaite are compared in Table 6.

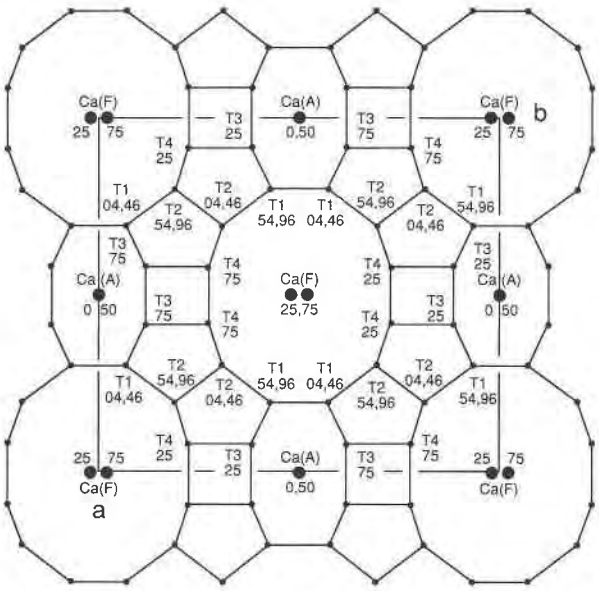

Fig. 1. Projection of the structure of Ca-rich mordenite on (001), drawn from the atomic coordinates reported by Elsen et al. (1987), but with the anion positions omitted for clarity. Numbers are z coordinates × 100.

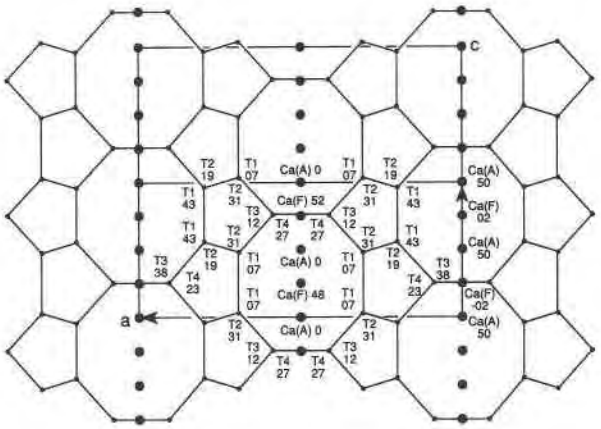

Fig. 2. Projection of the structure of Ca-rich mordenite from y = 0–½ on (010), with the anion positions omitted. Two unit cells along [001] are shown. Numbers are y coordinates × 100.

The mordenite framework has a two-dimensional channel system consisting of three channel types: a set of eight-membered-ring channels and a set of 12-membered-ring channels, both of which run parallel to **c** and which alternate with one another in the **a** and **b** directions (Fig. 1), and a set of eight-membered-ring channels parallel to **b**, which are very short and which connect the two types of **c**-axis channels along [010]. The **b**-axis channels are so short, being only one four-membered-ring long, that they are often called side pockets. They appear in projection in Figure 2 as rows of eight-membered rings (the channel mouths or ports) stacked along [001]. In Ca-rich mordenite both types of **c**-axis channels are occupied by H_2O molecules and by Ca^{2+} ions in the A and F sites. The Ca(A) are located in the eight-membered-ring **c**-axis channels and are coordinated to six framework O atoms plus two H_2O molecules, and the Ca(F) are in the 12-membered-ring channels, where they are coordinated to seven H_2O and no framework anions. The Ca ions are completely and readily exchangeable with a variety of other monovalent and divalent cations, and the structure can be dehydrated partially or completely up to 800 °C, which is the upper limit of its stability.

In contrast to mordenite, maricopaite has only a one-dimensional channel system consisting of two channel types, one of which is permanently obstructed. (However, single-ring interchannel ports may allow some diffusion in a second dimension.) The 12-membered-ring elliptical channels parallel to **c** in mordenite are retained in maricopaite but have a somewhat different shape in cross section (Fig. 3). The maximum free dimensions of the maricopaite channel are ca. 5.4 (‖**a**) and 7.2 Å (‖**b**). These were obtained by assuming a radius of 1.35 Å for $^{[2]}O^{2-}$ (Shannon, 1976) and drawing appropriately scaled circles, centered on the anion sites that define the boundary of one of the 12-membered-ring channels in an enlarged section of Figure 3.

The second channel type in maricopaite consists of unusually shaped 12-membered-ring channels, which are parallel to **c** and which appear in projection in Figure 3 as cruciform polygons defined by the T8, T4, T3, T6, T5, and T7 nodes. These unique cruciform channels correspond to the eight-membered-ring **c**-axis channels of mordenite reconfigured into 12-membered-ring channels by the loss of the T4-T4 and T5-T5 tetrahedral linkages, i.e., by the framework interruptions at these points. This leaves T4 and T5 tetrahedra as the only threefold-con-

Table 6. Comparison of chemical and crystallographic data for Ca-rich mordenite and maricopaite

	Ca-rich mordenite	Maricopaite
Cell contents	$Ca_{3.4}Al_{7.8}Si_{40.2}O_{96}\cdot xH_2O$	$Pb_{7.2}Ca_{2.2}Al_{11.6}Si_{36.4}O_{99.6}\cdot 32H_2O$
Si/Al ratio	5.13	3.14
Framework ρ	17.3	16.6
Unit cell	a = 18.091(4), b = 20.418(4)	a = 19.434(2), b = 19.702(2)
	c = 7.508(1) Å, V = 2773.3 Å³	c = 7.538(1) Å, V = 2886.1 Å³
Space group	*Cmcm*	*Cm2m* (pseudo-*Cmcm*)
Crystal habit	acicular	acicular

Note: data for Ca-rich mordenite are taken from Elsen et al. (1987). The unit-cell contents are derived from electron microprobe analyses rather than the crystal-structure analysis results.

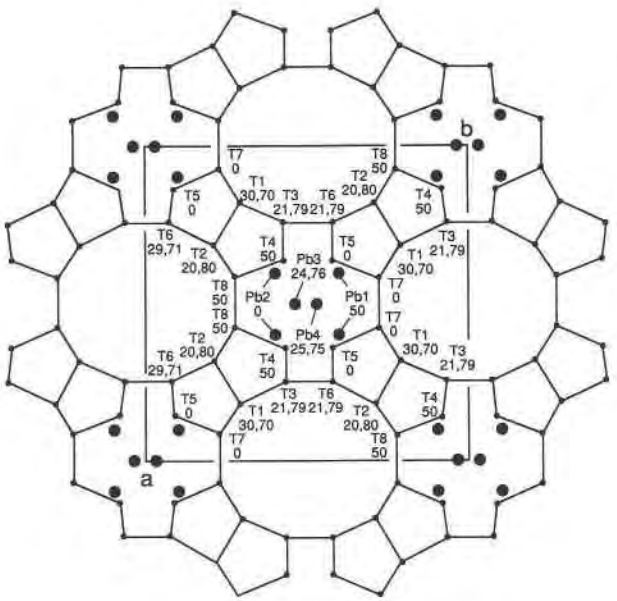

Fig. 3. Projection of the structure of maricopaite on (001), also with the anion positions omitted. Numbers are z coordinates × 100. Note that the cell origin should be shifted by ½ along the **a** axis to facilitate comparison with the mordenite structure in Fig. 1.

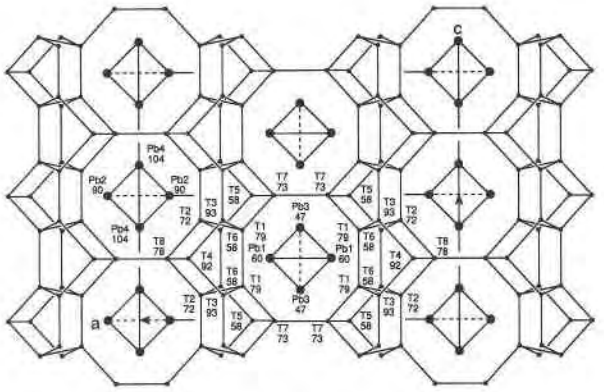

Fig. 4. Projection of the structure of maricopaite from y = ½–1 on (010), with the anion positions omitted. Two unit cells along [001] are shown, this portion of the structure being directly analogous to that part of the mordenite structure in Fig. 2. Numbers are y coordinates × 100.

nected tetrahedra in the structure. The broken linkages destroy the mordenite-type four-membered rings (defined by T8-T4 ... T4-T8 and T7-T5 ... T5-T7 in Fig. 3), and, in effect, the four- and eight-membered rings merge, producing the cruciform polygons in Figure 3. The free dimensions of the cruciform channels are ca. 5.2 (‖**a**) and 2.8 Å (‖**b**).

A second consequence of the loss of the four-membered rings is the destruction of the very short eight-membered-ring channels that run parallel to **b** in mordenite and that connect the two types of **c**-axis channels in that mineral. Instead, the mordenite-type elliptical 12-membered-ring and the cruciform 12-membered-ring channels of maricopaite are directly connected to one another through single eight-membered-ring ports, which appear in rows parallel to [001] in Figure 4. Each port, which has free dimensions of ca. 5.0 (‖**a**) and 5.5 Å (‖**c**), is simply the one surviving end of a mordenite-type **b**-axis channel. Comparison of Figures 2 and 4 shows that the mordenite and maricopaite structures are essentially the same in this projection, except that the components of the multiple five-membered-ring chains parallel to **c** are superimposed in mordenite but are slightly displaced from one another along **a** in maricopaite.

The anions *O*3 and *O*9, which would constitute the T4-T4 and T5-T5 linkages in a fully connected tectosilicate framework, are shifted into the cruciform channels, where their valence requirements are satisfied by bonding to the Pb atoms located there. Thus positioned, O3 and O9 permanently obstruct the cruciform channels in the [001] direction. The Pb atoms are therefore prevented from diffusing through the channels in this direction but might conceivably escape through the eight-membered-ring ports into the elliptical 12-membered-ring channels, which are unobstructed except for mobile (presumably) H_2O molecules. The channel-obstructing role of O3 and O9 is evident in Figure 5, which shows the anions bordering the channels as circles of radius 1.35 Å. Atom O3 has the largest displacement factor [B_{iso} = 3.8(5) Å^2] of any framework anion, a fact that might be considered evidence for the positional disorder of this atom. Such disorder would not be unexpected in view of the fact that O3 is bonded to the partially vacant cation sites Pb1, Pb3, and Pb4. However, the other unshared anion, *O*9, has a more modest B_{iso} of 2.4(4) Å^2, despite being bonded to Pb on partially vacant sites, and the mean B_{iso} value for framework anions (plus O19w) bonded to Pb differs insignificantly from the mean for those anions bonded only to T atoms, i.e., 2.5 vs. 2.6 Å^2.

Extraframework cations

The second unique structural feature of maricopaite, the first being the highly unusual shape of the cruciform channels, is the nature of the extraframework cation species. Unlike naturally occurring mordenite and all other natural zeolites, maricopaite contains no alkali or alkaline earth metal ions. It is the only natural zeolite having Pb as the dominant large cation, but what really sets maricopaite apart from the rest is the clustering of Pb atoms into Pb_4 tetrahedral groups. These are positioned in the centers of the cruciform channels in Figure 3 and in the centers (in projection) of the eight-membered ring windows in Figure 4. Figure 3 also shows that there are two alternative sites for the Pb_4 tetrahedron, sites that cannot be simultaneously occupied because of short Pb-Pb distances. Specifically, the distances Pb3–Pb4 = 1.377(7), Pb2–Pb3 = 2.929(4), and Pb1–Pb4 = 2.986(6) Å are all impossibly short, if one accepts a Pb-Pb separation of 3.4 Å as the minimum distance possible (Bengtsson and

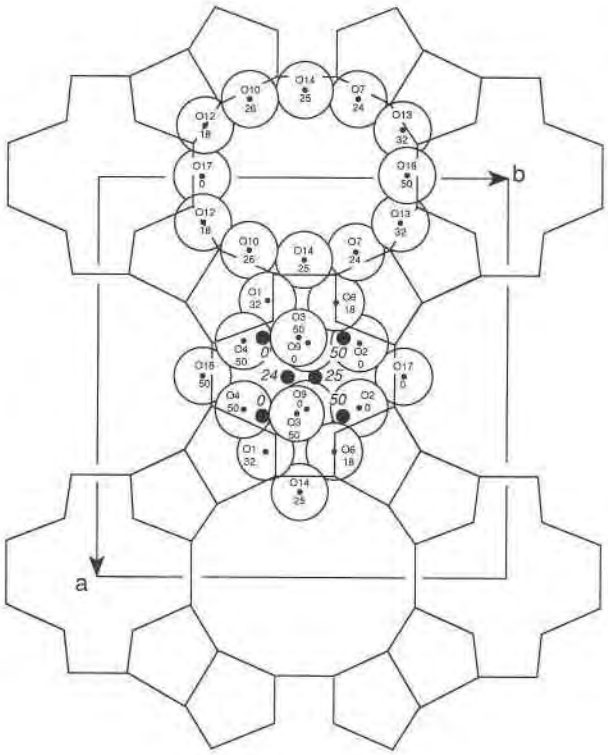

Fig. 5. A section of Fig. 3 from $z = 0$–½, showing the bordering anions and enclosed Pb atoms for two of the channels. The anions are represented as circles drawn assuming a radius of 1.35 Å for $^{[2]}O^{2-}$. Note that the cruciform 12-membered-ring channels are permanently obstructed by the unshared framework anions *O*3 (bonded to T4) and *O*9 (bonded to T5). Numbers are z coordinates × 100.

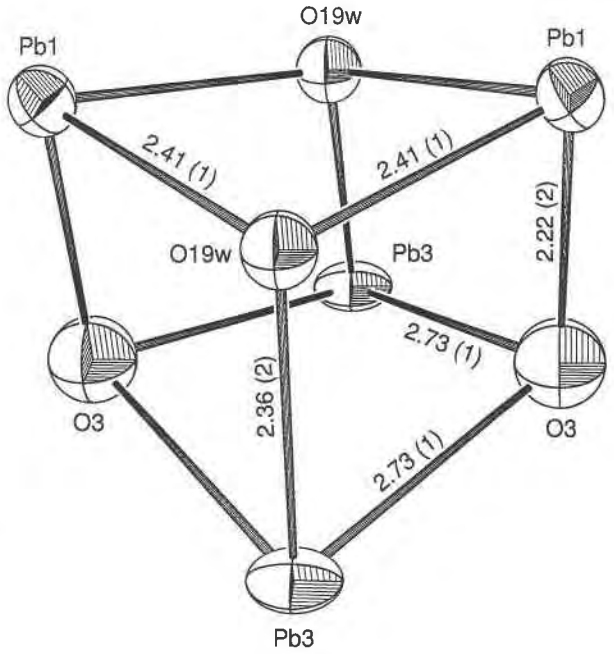

Fig. 6. An ORTEP plot of a $Pb_4(O,OH)_4$ group composed of a $Pb1_2Pb3_2$ tetrahedron and its four capping ligands O3 (× 2) and O19w (× 2).

Holmberg, 1990). In effect, maricopaite contains two different Pb_4 tetrahedra, which will henceforth be designated as $Pb1_2Pb3_2$ and $Pb2_2Pb4_2$, after their constituent atoms. Atoms Pb3 and Pb4 form a split-atom pair, which is symmetrically disposed about the mordenite-type A sites at ~(0,0,±¼) and their *C*-centered equivalents. Within the $Pb1_2Pb3_2$ and $Pb2_2Pb4_2$ tetrahedra the mean interatomic distances are 3.865 and 3.804 Å, respectively, with a range of 3.788(3)–3.954(4) Å (Table 5). The minimum distances between tetrahedra are even shorter: 3.584(4) and 3.745(16) Å for Pb3-Pb3 and Pb4-Pb4, respectively.

The Pb atoms of maricopaite are each bonded to six to eight framework anions and H_2O molecules (Table 5), taking 3.25 Å as the maximum Pb-O separation that can be considered to be a bonding distance. An ORTEP plot (Johnson, 1976) of the $Pb1_2Pb3_2$ tetrahedron and its nearest anion neighbors appears in Figure 6. The three Pb atoms that define each tetrahedron face are mutually coordinated to one anion situated above each face; e.g., each $Pb1_2Pb3$ face is capped by an O19w (an extra-framework anion) and each $Pb3_2Pb1$ face is capped by an O3 (one of the unshared framework O atoms). Inspection of Table 5 shows that, except for Pb3-O3, all of the Pb-O distances involved are the shortest in the structure, ranging from 2.22(2) to 2.41(1) Å. All other Pb-O distances in the table are ≥2.7 Å. The short Pb-capping ligand distances in maricopaite are similar to the Pb-O bond lengths in orthorhombic and tetragonal PbO, namely 2.221(2), 2.245(2), and 2.481(2) (× 2) (Hill, 1985) and 2.31 (× 4) Å (Leciejewicz, 1961), respectively. The shortness of these distances is associated with a high degree of covalency in the Pb-O bond (Trinquier and Hoffmann, 1984; Evarestov and Veryazov, 1991a, 1991b).

The $Pb1_2Pb3_2$ tetrahedron and its face-capping ligands O3 and O9 together constitute a $Pb_4(O,OH)_4$ group that is chemically and structurally analogous to the $Pb(OH)_4$ groups in $[Pb_4(OH)_4]_3(CO_3)(ClO_4)_{10}\cdot 6H_2O$ (Hong and Olin, 1973) and $[Pb_4(OH)_4](ClO_4)_4\cdot 2H_2O$ (Hong and Olin, 1974). In addition, $Pb_3O(OH)_3$ clusters similar to $Pb_4(OH)_4$ but having one vacant Pb site have been produced by ion exchange within the sodalite cages of zeolite 4A (Ronay and Seff, 1993). The relevant Pb-O distances in all three structures are, with one exception, close to those in the $Pb_4(O,OH)_4$ group in maricopaite, i.e., 2.29(2)–2.54(3) Å in the perchlorates and 2.3(1)–2.82(9) Å in the zeolite, with additional, longer distances to O atoms that are not part of the clusters. Likewise, the intracluster Pb-Pb distances in maricopaite [3.788(3)–3.954(4) Å] are similar to those in the perchlorates [3.721(2)–3.945(2) Å] and the zeolite (3.94 Å). All fall toward the higher end of the range of shortest Pb-Pb distances in lead oxides and hydroxides listed in the review paper of Bengtsson and Holmberg (1990).

The structure of $Pb_4O[Pb_2(BO_3)_3Cl]$ contains Pb_4O groups, with the O atom being located at the center of a

Pb_4 tetrahedron (Behm, 1983). The intracluster Pb-Pb and Pb-O distances [3.702(2)–3.817(2) and 2.26(1)–2.35(2) Å, respectively] are similar to those in maricopaite, and there is also a very short Pb-Pb distance of 3.548(2) Å between adjacent Pb_4O tetrahedra, which is similar to the Pb3-Pb3 distance of 3.584(4) Å between adjacent $Pb1_2Pb3_2$ tetrahedra in maricopaite. These two short distances are only slightly longer than the minimum in Pb metal, 3.50 Å.

A situation analogous to that described above for the $Pb1_2Pb3_2$ tetrahedron in maricopaite exists for its alternative, the $Pb2_2Pb4_2$ tetrahedron. In the latter case, each $Pb4_2Pb2$ face is capped by an O9 atom, and each $Pb2_2Pb4$ face probably by O28w, although the latter atom is one of those poorly defined channel atoms whose validity is not above question.

Ronay and Seff (1993) noted that the two polynuclear complexes $[Pb_3(OH)_4]^{2+}$ and $[Pb_4(OH)_4]^{4+}$ are "the predominant lead-containing species in nondilute near-neutral aqueous solutions of Pb^{2+}," with the tetranuclear complex being dominant at slightly alkaline pH. Johansson and Olin (1968) studied the structure of $[Pb_4(OH)_4]^{4+}$ in hydrolyzed Pb^{2+} perchlorate solutions by X-ray scattering and found the capped tetrahedral configuration described above, with a Pb-Pb distance of 3.85 Å and a mean Pb-O distance of 2.6 Å, both comparable with those in maricopaite and the various synthetic compounds just described. A Pb-Pb separation of 3.85 Å is 10% longer than the minimum distance of 3.50 Å in Pb metal, but Maroni and Spiro (1968) found that they could only interpret the infrared and Raman spectra of $[Pb_4(OH)_4]^{4+}$ by assuming an attractive interaction between Pb atoms of the complex. This implies the existence of weak metal-metal bonding in maricopaite and, if true, would make this extraordinary mineral a zeolitic metal-cluster compound. In addition to its occurrence as a cationic complex in crystalline solids and aqueous solution, the capped Pb_4X_4 tetrahedron exists in the gas phase as neutral Pb_4O_4 molecules that are isoelectronic with $[Pb_4(OH)_4]^{4+}$ (Ogden and Ricks, 1972; Khanna and Park, 1986).

The fact that $[Pb_4(OH)_4]^{4+}$ is the dominant Pb^{2+} species in aqueous solution at neutral to slightly alkaline pH suggests a possible answer to the question of why maricopaite crystallized with an interrupted mordenite-like framework instead of simply adopting the standard mordenite structure. The latter is, after all, a stable, commonly occurring entity capable of accommodating a large variety of cations (Gottardi and Galli, 1985; Tyburce et al., 1991). Reference to Figure 3 shows that $Pb1_2$ and $Pb2_2$ pairs (which are tetrahedron edges) occur at the very points where the framework interruptions occur, i.e., between T5 and T5 and between T4 and T4, respectively. It is suggested that maricopaite crystallized around the $[Pb_4(OH)_4]$ complexes that already existed in the formative solution, and that the framework discontinuities result from the necessity to accommodate these large structural units in the rather small eight-membered-ring c-axis channels of a mordenite-type framework. This would be akin to the templating role of some organic ions and molecules in determining which zeolite framework crystallizes from solutions containing these entities (Mortier and Schoonheydt, 1985).

In addition to Pb, the electron microprobe analysis of maricopaite (Peacor et al., 1988) indicates the presence of a lesser amount of Ca, the calculated extraframework cation content being $Pb_{7.2}Ca_{2.2}$ per cell, and yet no separate Ca site was found by structure analysis. Several explanations for this missing Ca are possible: (1) The Ca atoms are disordered over the sites predominantly occupied by Pb; i.e., there is Pb-Ca solid solution. (2) The Ca content of maricopaite is quite variable, with the crystal used for structure analysis containing little or none of that element. (3) The missing Ca is disordered over multiple sites in the elliptical 12-membered-ring channels to such a degree that it is unlocatable by X-ray diffraction methods. Refinement of Pb site occupancy factors, assuming Pb as the only element present, yielded 7.5 Pb per cell. This is close to the value of 7.2 Pb from the electron microprobe analysis, but the former value could still conceal within it the 2.2 Ca atoms, which have a combined X-ray scattering power equivalent to ~0.5 Pb atom. A Ca-free crystal seems unlikely, given the fact that maricopaite crystallized in a Ca-rich environment, namely a calcite-fluorite vein. In our opinion, the most probable explanation is Ca disorder over multiple sites in the main channel. This has a precedent in the structure of natural mordenite, where most of the Na^+ and K^+ ions indicated by chemical analysis are unlocatable by structure analysis, their apparent absence being ascribed to extensive positional disorder (Meier, 1961; Alberti et al., 1986).

Extraframework anions

All the remaining occupied extraframework sites in maricopaite (denoted by Ow in the tables) occur within the structural channels and most are situated fairly near standard extraframework sites in mordenite. Except for O19w and O28w, whose bond-valence sums in Table 7 imply that they are OH groups (at least part of the time), all presumably contain H_2O molecules. The refined site occupancies for the Ow sites in Table 3 correspond to a total of $19(H_2O + OH)$ per cell, compared with the $32(H_2O + OH)$ per cell indicated by the TGA analysis of maricopaite (Peacor et al., 1988). However, little weight should be attached to this discrepancy, as the hydration state of maricopaite is probably variable and the estimated standard deviations of the refined occupancy factors of the Ow sites are quite large. Indeed, except for O19w, which appeared as a small peak in the *E* map and which behaved much like the framework anions during the refinement, all of the Ow are somewhat suspect. This is so because they were derived solely from the last two difference syntheses, where they appeared among the largest, but still very small (≤ 2.5 e/Å^3), peaks. Given the abundance of spurious peaks in difference syntheses (Hu and Depmeier, 1992), especially in the vicinity of heavy

atoms like Pb, it is best to regard all Ow sites except O19w as tentative.

The Ow sites located within the cruciform channels, namely O19w, O26w, O27w, and O28w, cannot be fully occupied owing to their proximity to the Pb sites, which are also partially vacant. We propose that these Ow atoms act as replacements for their associated Pb atoms, filling sites very near the cation positions when the latter are vacant. The Pb-Ow pairs associated in this way are Pb1 + O27w, Pb2 + O26w, Pb3 + O28w, and Pb4 + O19w. There is a precedent for such a situation in other zeolite structures, e.g., in the natural mordenite studied by Alberti et al. (1986), where the extraframework B site is occupied 50% by K^+ and 50% by H_2O.

Chemical formula and the presence of OH

In addition to the question of the number of H_2O + OH per cell, there is some residual uncertainty concerning the rest of the formula of maricopaite, centered on the relationship between Pb and OH. The empirical unit-cell contents derived from the combined electron microprobe and TGA analyses of Peacor et al. (1988) and normalized to 48 T atoms per cell, as indicated by the structure analysis, are

$$Pb_{7.2}Ca_{2.2}Al_{11.6}Si_{36.4}O_{99.6}\cdot 31.8H_2O. \quad (1)$$

Rounding off coefficients yields

$$Pb_7Ca_2Al_{12}Si_{36}O_{100}\cdot 32H_2O \quad (2)$$

which has an excess of two negative charges. The indicated number of O atoms agrees exactly with the 100 framework anions found in the structure analysis, but eight of them, namely the unshared tetrahedral vertex anions *O*3 and *O*9, are almost certainly sites containing O and OH. This is so because they are both bonded to several Pb atoms, and when most of their associated Pb sites are vacant because of disorder, O3 and O9 must bond to H to fill their valence requirements. This is evident in Table 7, which shows that the bond valence sums of O3 and O9 have normal values of 2.2 and 2.1 vu, respectively, in the presence of their associated Pb_4 tetrahedron, but only 1.4 vu in its absence. Specifically, O3 is an O^{2-} when the $Pb1_2Pb3_2$ tetrahedron is present and an $(OH)^-$ when it is absent. An analogous situation will exist for O9 when the $Pb2_2Pb4_2$ tetrahedron is present or absent. The bonding of H to terminal (unshared) O atoms of the framework has ample precedents among the known interrupted framework silicates. Of the ten such structures listed by Smith (1988), seven contain such terminal OH groups.

Additional OH exists in maricopaite at the extraframework sites O19w and (possibly) O28w, as indicated by their bond valence sums of 1.40 and 0.55 vu, respectively. These values might be interpreted to mean that O19w is an OH,O site and O28w OH,H_2O site, but given the estimated standard deviations of the Pb-Ow distances and the possibility that some of those distances are virtual, this interpretation is speculative.

TABLE 7. Empirical bond valence sums (vu) for maricopaite

Cations*		Framework anions		Extraframework sites	
Pb1	2.12	*O*1	2.23	O19w	1.40
Pb2	1.58	*O*2	1.97	O20w	0.13
Pb3	1.54	*O*3**	2.17, 1.41	O21w	—
Pb4	1.05	*O*4	1.97	O22w	—
*T*1	4.26	*O*5	2.02	O23w	—
*T*2	4.18	*O*6	1.99	O24w	—
*T*3	3.88	*O*7	1.95	O25w	—
*T*4	4.17	*O*8	2.15	O26w	0.17
*T*5	4.00	*O*9**	2.13, 1.45	O27w	0.10
*T*6	3.87	*O*10	1.99	O28w	0.55
*T*7	3.96	*O*11	2.18		
*T*8	3.91	*O*12	2.05		
		*O*13	2.11		
		*O*14	1.91		
		*O*15	2.17		
		*O*16	2.10		
		*O*17	2.16		
		*O*18	1.96		

* Valences involving the T atoms are calculated assuming 26.4% Al and 73.6% Si on all T sites except T5, which is assumed to be 100% Si. The virtual distance of 2.04 Å for Pb4-O28w is ignored.

** For *O*3, the first sum is for coordination by T4, Pb1, and 2Pb3 [i.e., when the $Pb1_2Pb3_2$ tetrahedron is present], and the second sum is for coordination by T4 and 2Pb4 [when the $Pb2_2Pb4_2$ tetrahedron is present]. For *O*9, the first sum is for coordination by T5, Pb2, and 2Pb4 [when the $Pb2_2Pb4_2$ tetrahedron is present], and the second sum is for coordination by T5 and 2Pb3 [when the $Pb1_2Pb3_2$ tetrahedron is present]. Bond valence calculations based on the parameters of Brese and O'Keeffe (1991).

In view of the above considerations, Formula 2 should be rewritten as

$$Pb_7Ca_2Al_{12}Si_{36}(O,OH)_{100}\cdot n(H_2O,OH) \quad (3)$$

where O,OH represents the framework anions, H_2O,OH the extraframework species, and n the uncertainty in the amount of OH present. That is, the 32 H_2O per cell lost between 20 and 500 °C during the TGA analysis of Peacor et al. (1988) represents both H_2O molecules and OH. The crystal structure analysis does not give an unambiguous answer as to how this H_2O is to be apportioned between the two species, and thus the simplified Formula 3 is the best approximation that can be given at this time.

Lastly, mention should be made of the small (0.5 wt%) hydrocarbon content of maricopaite reported by Peacor et al. (1988). Scarcity of material precluded tests to identify the organic compounds present, and the crystal structure analysis yielded no additional information on the subject. The organic component, if present in the crystal used for the structure analysis, is presumably in the form of molecules or perhaps organic ions bonded to some of the extraframework cations. Like the Ca ions, they may be so disordered in the channels as to be unlocatable by X-ray diffraction.

ACKNOWLEDGMENT

Contribution no. 492, the Mineralogical Laboratory, Department of Geological Sciences, the University of Michigan.

REFERENCES CITED

Alberti, A., Davoli, P., and Vezzalini, G. (1986) The crystal structure refinement of a natural mordenite. Zeitschrift für Kristallographie, 175, 249–256.

Behm, H. (1983) Hexalead chloride triorthoborate oxide, $Pb_4O[Pb_2(BO_3)_3Cl]$. Acta Crystallographica, C39, 1317–1319.

Bengtsson, L., and Holmberg, B. (1990) Cationic lead (II) hydroxide complexes in molten alkali-metal nitrate. Journal of the Chemical Society, Faraday Transactions, 86, 351–359.

Brese, N.E., and O'Keeffe, M. (1991) Bond-valence parameters for solids. Acta Crystallographica, B47, 192–197.

Elsen, J., King, G.S.D., and Mortier, W.J. (1987) Influence of temperature on the cation distribution in calcium mordenite. Journal of Physical Chemistry, 91, 5800–5805.

Estermann, M., McCuskser, L.B., Baerlocher, C., Merrouche, A., and Kessler, H. (1991) A synthetic gallophosphate molecular sieve with a 20-tetrahedral-atom pore opening. Nature, 352, 320–323.

Evarestov, R.A., and Veryazov, V.A. (1991a) The electronic structure of crystalline lead oxides. I. Crystal structure and LVC-CNDO calculations. Physica Status Solidi B, 165, 401–410.

——— (1991b) The electronic structure of crystalline lead oxides. II. Chemical bonding in the crystalline lead oxides. Physica Status Solidi B, 165, 411–418.

Gottardi, G., and Galli, E. (1985) Natural zeolites, p. 225–233. Springer-Verlag, Berlin.

Harrison, W.T.A., Gier, T.E., and Stucky, G.D. (1991) Synthesis and crystal structure of a novel beryllium phosphate open-framework structure. Journal of Materials Chemistry, 1, 153–154.

Harrison, W.T.A., Martin, T.E., Gier, T.E., and Stucky, G.D. (1992) Tetrahedral-atom zincophosphate structures: Synthesis and structural characterization of two novel anionic eight-ring frameworks containing cationic 1,4-diazabicyclo[2.2.2]octane guests. Journal of Materials Chemistry, 2, 175–181.

Hill, R.J. (1985) Refinement of the structure of orthorhombic PbO (massicot) by Rietveld analysis of neutron powder diffraction data. Acta Crystallographica, C41, 1281–1284.

Hong, S.-H., and Olin, Å. (1973) On the crystal structure of $[Pb_4(OH)_4]_3(CO_3)(ClO_4)_{10}\cdot 6H_2O$. Acta Chemica Scandinavica, 27, 2309–2320.

——— (1974) The crystal structure of $[Pb_4(OH)_4](ClO_4)_4\cdot 2H_2O$. Acta Chemica Scandinavica A, 28, 233–238.

Hu, X., and Depmeier, W. (1992) Pitfalls in the X-ray structure determination of pseudosymmetric sodalites, and possibly zeolites. Zeitschrift für Kristallographie, 20, 99–111.

Ito, M., and Saito, Y. (1985) The crystal structure of ion-exchanged mordenite. Bulletin of the Chemical Society of Japan, 58, 3035–3036.

Johansson, G., and Olin, Å. (1968) On the structures of the dominating hydrolysis products of lead (II) in solution. Acta Chemica Scandinavica, 22, 3197–3201.

Johnson, C.K. (1976) OR TEP-II: A Fortran thermal-ellipsoid plot program for crystal structure illustrations. ORNL-5138, Oak Ridge National Laboratory, Oak Ridge, Tennessee.

Khanna, R.K., and Park, Y.J. (1986) Infrared and Raman spectra of matrix isolated lead oxide species. Structure of Pb_2O_2 and Pb_4O_4. Spectrochimica Acta, 42A, 603–606.

Leciejewicz, J. (1961) On the crystal structure of tetragonal (red) PbO. Acta Crystallographica, 14, 1304.

Maroni, V.A., and Spiro, T.G. (1968) Vibrational analysis for polynuclear hydroxylead (II) complexes. Inorganic Chemistry, 7, 188–192.

Meier, W.M. (1961) The crystal structure of mordenite (ptilolite). Zeitschrift für Kristallographie, 115, 439–450.

Mortier, W.J., and Schoonheydt, R.A. (1985) Surface and solid state chemistry of zeolites. Progress in Solid State Chemistry, 16, 1–125.

North, A.C.T., Phillips, D.C., and Mathews, F.S. (1968) A semi-empirical method of absorption correction. Acta Crystallographica, A24, 351–359.

Ogden, J.S., and Ricks, M.J. (1972) Matrix isolation studies of Group IV oxides. IV. Infrared spectra and structures of PbO, Pb_2O_2, and Pb_4O_4. Journal of Chemical Physics, 56, 1658–1662.

Peacor, D.R., Dunn, P.J., Simmons, W.B., Wicks, F.J., and Raudsepp, M. (1988) Maricopaite, a new hydrated Ca-Pb, zeolite-like silicate from Arizona. Canadian Mineralogist, 26, 309–313.

Ronay, C., and Seff, K. (1993) Lead oxide hydroxide clusters in $Pb_9O(OH)_4$-A, zeolite A exchanged with Pb^{2+} at pH 6.0. Zeolites, 13, 97–101.

Shannon, R.D. (1976) Revised effective ionic radii and systematic studies of interatomic distances in halides and chalcogenides. Acta Crystallographica, A32, 751–767.

Smith, J.V. (1988) Topochemistry of zeolites and related materials. Chemical Reviews, 88, 149–182.

Trinquier, G., and Hoffmann, R. (1984) Lead monoxide. Electronic structure and bonding. Journal of Physical Chemistry, 88, 6696–6711.

Tyburce, B., Kappenstein, C., Cartraud, P., and Garnier, E. (1991) Effects of exchangeable cations on the absorption properties of Na^+ mordenite. Journal of the Chemical Society, Faraday Transactions, 87, 2849–2853.

Walker, N., and Stuart, D. (1983) An empirical method for correcting diffractometer data for absorption effects. Acta Crystallographica, A39, 158–166.

Manuscript received November 13, 1992
Manuscript accepted September 30, 1993